



Preparation of bismuth zeolitic imidazolate framework by laser ablation method in liquid

Negar Motakef Kazemi^{1,*} , Fereydoon Ataei² 

¹Department of Medical Nanotechnology, Faculty of Advanced Sciences and Technology, Tehran Medical Sciences, Islamic Azad University, Tehran, Iran.

²Laser Lab., Plasma Physics Research Center, Science and Research Branch, Islamic Azad University, Tehran, Iran.

*Corresponding author: motakef@iaups.ac.ir

Original Research

Abstract:

Received:
8 November 2023
Revised:
7 December 2023
Accepted:
12 December 2023
Published online:
10 March 2023

Zeolitic imidazolate framework (ZIF) is a new class of metal organic framework (MOF) with imidazolate ligands as linkers and metal ions as metal centers. A bismuth zeolitic imidazolate framework (Bi-ZIF) was prepared by laser ablation in liquid environment as a physical bottom-up method for the first time. The samples were characterized by Fourier transform infrared (FTIR) spectroscopy for evaluation of functional groups, X-ray diffraction (XRD) for determination of crystal structure, field emission scanning electron microscope (FESEM), and transmission electron microscope (TEM) for investigation of morphology and size of produced nanostructures. The antibacterial activity of samples was investigated by *Escherichia coli* (*E. coli*) as gram-negative bacterium and *Staphylococcus aureus* (*S. aureus*) as gram-positive bacterium. Based on the results, laser ablation is a quick, capable, clean, and simple candidate method for synthesizing different kinds of ZIF.

© The Author(s) 2024

Keywords: Bismuth zeolitic imidazolate framework; Laser ablation; Metal organic framework; Nanostructure

1. Introduction

Laser ablation is a very simple and clean top-down physical method to produce nanoparticles [1, 2]. This method has been used to develop alternative synthesis of materials in shorter times to produce smaller, uniform, and high-purity nanostructures in a liquid medium [1]. The ability of pulsed lasers in material processing and especially the role of lasers in production and modification of nanomaterials have been repeatedly investigated. Pulsed laser is an environmentally friendly green method with high purity nano products. The variety of control tools such as laser flux, wavelength, pulse width and spot size are the most important advantage of the pulsed laser ablation method for processing nanomaterials [3, 4].

Metal organic frameworks are hybrid organic inorganic frameworks or coordination polymer as porous materials [5, 6]. MOFs have attracted much attention due to their intrinsic properties [7, 8]. These nanostructures have shown potential applications in many fields [9–11] including luminescent [12], sensing [13], catalysis [14], storage [15, 16],

separation [17], sorbent [18, 19], drug delivery [20–22], cancer therapy [23], antibacterial [24–26], industrial usage [27]. Metal organic frameworks have been synthesized by different methods [28–32] including solution [33], solvothermal [34], hydrothermal [35], ionic liquids [36] microwave [37, 38], son chemical [39], diffusion [40], electrochemical [41], mechanochemical [42], laser ablation [43–45], combination of ultrasound and microwave [46]. Zeolitic imidazolate frameworks (ZIFs) are a subclass of MOFs with highly desirable properties and porous crystalline structures analogous to zeolites [47]. ZIFs are built by self-assembly metal ions and 4-connected nets of tetrahedral units through N atoms in imidazolate through several different synthesis routes [47–49]. Bismuth-based zeolitic organic framework is a metal organic framework with coordination-linked metal cages and the wide range of applications [50]. Based on the previous reports, laser abrasion was used to prepare MOFs based on zinc [51, 52], bismuth [53], copper [43], europium [44], zeolite imidazolate framework-67 (ZIF-67) [54], and copper imidazole [55]. This paper is the first detailed report on synthesizing bismuth zeolitic imidazolate

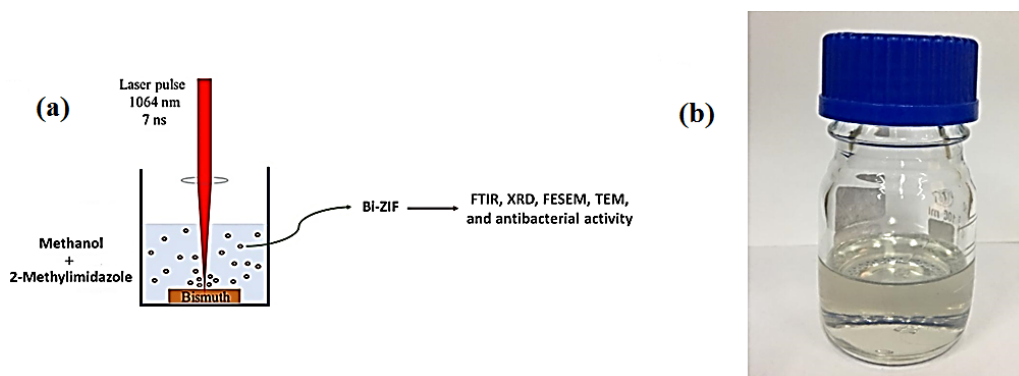


Figure 1. For MOF (a) scheme diagram of experimental setup, and (b) final sample with laser ablation method in liquid.

frameworks MOF by laser ablation method as quick, capable, easy, fast, and environmentally friendly method to synthesis.

2. Experimental procedure

A high purity (99%) bismuth bulk was irradiated by an Nd:YAG, Q-switched pulsed laser ($\lambda = 1064$ nm) with 7 ns pulse duration and a repetition rate of 10 Hz. Materials including bismuth target for preparation of Bi^{3+} ion as a connector center, 2-Methylimidazole (2MIm) as a bridging ligand, and methanol (MeOH) as a solvent were purchased

from Merck (Darmshtadt Germany).

Bismuth target was placed on the bottom of an open glass cylindrical vessel filled with 20 mL of 0.821 g 2MIm solution in methanol solvent. Height of liquid on the target was 6 mm. 2000 laser pulse was used to produce nanostructures in liquid environments with various 2MIm amount. Laser beam of 6 mm in diameter was focused on the surface of target by means of a 100 mm convex lens. Spot size of laser on the surface of target was estimated to be about 30 μm . The scheme and the final sample with laser ablation method in liquid are shown in Figure 1. There are 3 samples

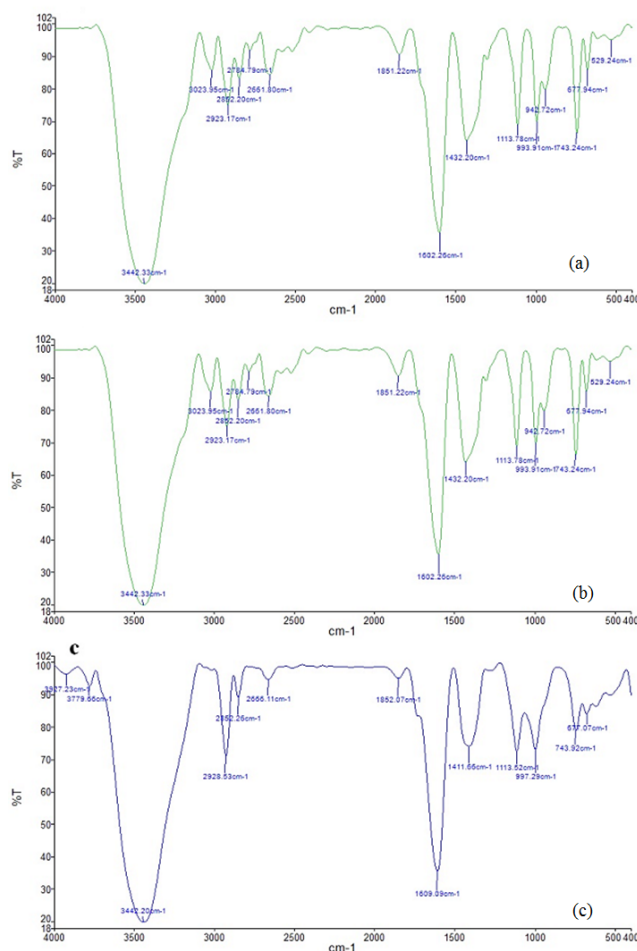


Figure 2. FTIR spectrum of samples at different ligand concentrations (a) 0.919 g, (b) 0.517 g, (c) and 1.642 g.

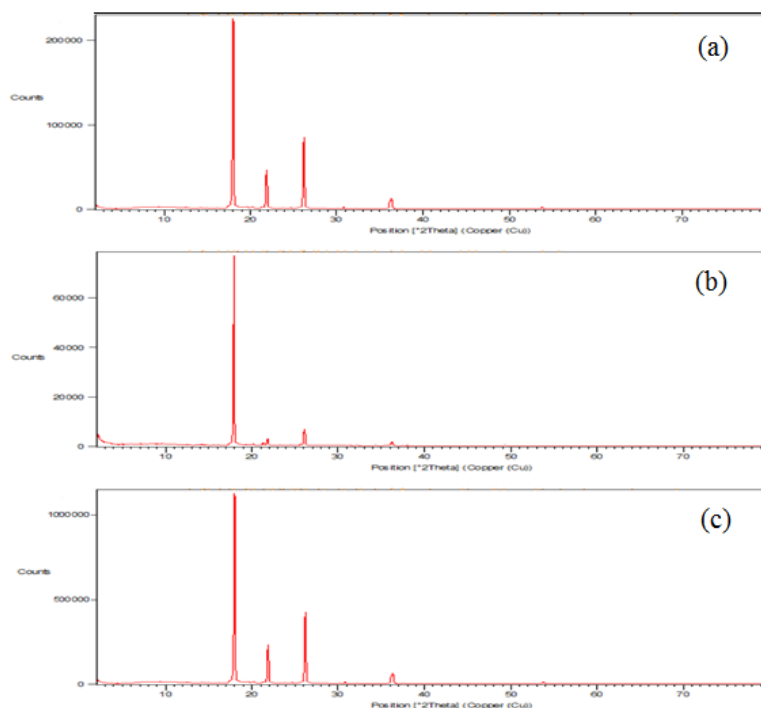


Figure 3. XRD pattern of samples at different ligand concentrations (a) 0.919 g, (b) 0.517 g, (c) and 1.642 g.

at different ligand concentrations of 0.517, 0.919, and 1.642 gr. As soon as the ablation starts, the solution changes its color and the precipitation of a solid occurs.

The samples were characterized by FTIR, XRD, FESEM, and TEM. Fourier transform infrared spectroscopy was used to determine the chemical bonds of samples by Spectrum Two FTIR Spectrometer from PerkinElmer. X-ray diffraction pattern was employed for investigation of crystalline structures of samples by dried suspensions on Si substrate. X-ray diffraction patterns were recorded by STOE X-ray diffractometer with Cu $K\alpha$ radiation ($\lambda = 1.54060 \text{ \AA}$). Morphology and size of samples were evaluated by FESEM (SIGMA VP) and TEM (EM10C) microscopes from Zeiss Company. To take FESEM images, few drops of suspensions were dried on silicon substrate and coated with gold thin film. For TEM images few drops of suspensions were dried on carbon-coated copper grids. The antibacterial activity was evaluated by disk diffusion method against *Escherichia coli* as gram-negative bacteria (ATCC 25922) and *Staphylococcus aureus* as gram-positive bacteria (ATCC

25923).

3. Results and discussion

FTIR spectra of samples were shown in Figure 2 in the range of $400 - 4000 \text{ cm}^{-1}$ with KBr pellets at different concentration of ligand. The band of about 3442 cm^{-1} is assigned to asymmetric stretching of the C-H methyl group. The observed peak due to C=N stretching is about 1602 cm^{-1} , while the peak at about 1432 cm^{-1} is corresponded to the entire traction loop. The adsorption bands at 1113 and 993 cm^{-1} are attributed to C-N stretching and bending, respectively. The aromatic bending of sp^2 C-H appeared at 743 and 677 cm^{-1} [56]. The adsorption bands at 529 cm^{-1} are appeared to Bi-N stretching, which bonded zinc to nitrogen atoms of the linkers to form a porous ZIF coordination structure [53].

X-ray diffraction patterns of nanostructures in the range of $2\theta = 5^\circ - 80^\circ$ are presented in Figure 3. XRD patterns of samples were recorded under the low-dose liquid condition by drying a few drops of the suspension on a silicone sub-

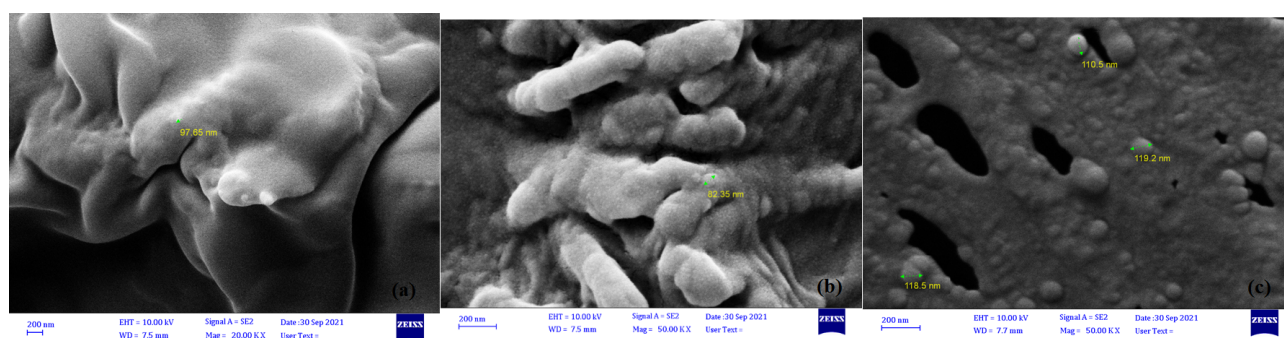


Figure 4. FESEM images of samples at different ligand concentrations (a) 0.919 g, (b) 0.517 g, (c) and 1.642 g.

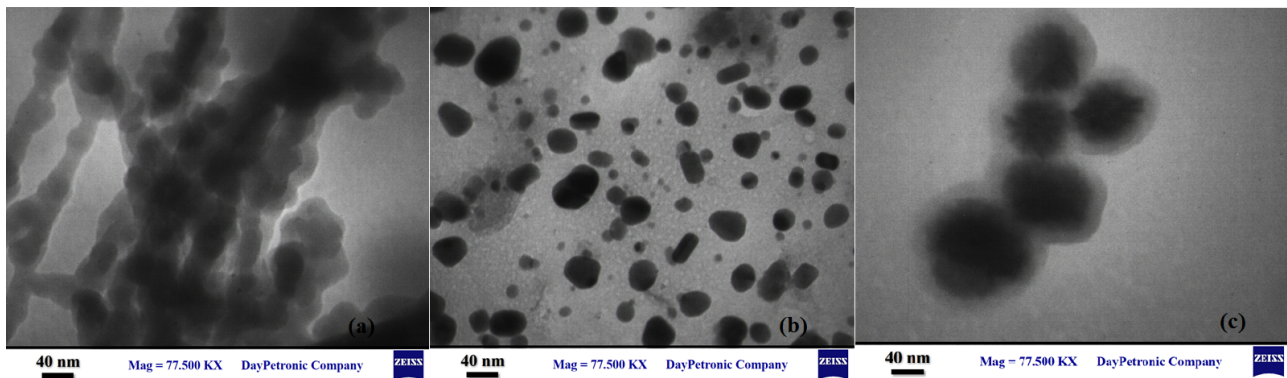


Figure 5. TEM images of samples at different ligand concentrations (a) 0.919 g, (b) 0.517 g, (c) and 1.642 g.

strate. The peaks are located at 2θ about 18° , 22° , and 26° , which correspond to the (222), (114), and (134) planes respectively. The intensity of the peaks depends on the angle of irradiation and the number of samples. The intensity of the peaks increased with the increase in the concentration of the ligand in the liquid environment due to the increase of the number of samples. The XRD patterns are in good agreement with the presented patterns in previous reports [57].

Field emission scanning electron microscope images of nanostructures are shown at different ligand concentrations in Figure 4. According to the results, with increasing concentration, the morphology changes from rod to spherical and the number of nanostructures increases.

Transmission electron microscope images of nanostructures are shown at different ligand concentrations in Figure 5. The spherical nanoparticles with sizes of 82, 98, and 120 nm were observed in concentrations of 0.517, 0.919, and 1.642 gr, respectively. Based on the results, the size of nanostructures generally increases with increasing concentration.

Serial dilution titration method was used to determine the minimum inhibitory concentration (MIC) and the minimum bactericidal concentration (MBC) to evaluate the antibacterial activity of different solutions. The MHB (Mueller Hinton Broth) medium was used overnight for the growth of *Staphylococcus aureus* and *Escherichia coli* at 37°C . Double serial dilutions were added to give the final inoculation of 5×10^5 colony-forming units (CFU)/mL. MIC and MBC of samples were determined at 37°C for 24 h (Table 1).

According to the MBC/MIC ratio, antibacterial activity can be evaluated, which is in the $\text{MBC/MIC} \leq 4$ ratio as bacte-

ricidal and in $\text{MBC/MIC} > 4$ as bacteriostatic effect. Based on the results, the samples are bactericidal. Increasing the concentration has no effect on the antibacterial properties of two initial concentration samples and the third sample does not have antibacterial properties. Based on the results, the concentration of 0.517 and 0.919 gr of ligand has the same antibacterial properties. The main mechanisms of MOF antibacterial activity include direct contact with cell walls and bacterial cell destruction, generation of reactive oxygen species (ROS), and release of antimicrobial ions [58]. This MOF can release bismuth ions and act as an antibacterial agent. According to the results, by increasing the size to 120 nm in a concentration of 1.642 gr, antibacterial property was not observed due to the impossibility of entering the bacteria. The results confirm the previous report [55].

4. Conclusion

For the first time, the nano-sized Bi-ZIF was synthesized by laser ablation method in liquid conditions. Pulsed laser ablation was investigated as a new method for the synthesis of bismuth zeolite imidazolate framework by bismuth target irradiation in 2-methylimidazole solution with methanol as the liquid environment of ablation at different ligand concentrations. X-ray diffraction patterns confirm that MOF nanostructures have been successfully synthesized in all samples. Fourier transform analysis identified functional groups in samples produced at different ligand concentrations. TEM and SEM images show that MOF nanostructures were prepared. Antibacterial properties of the sample were also observed due to the presence of bismuth ion. Therefore, the laser ablation method as an easy, fast, and friendly environmental method has a wide application potential in nanotechnology.

Table 1. MIC and MBC of samples

Ligand content (gr)	Strains			
	<i>E. Coli</i> (ATCC 25922)		<i>S. aureus</i> (ATCC 25923)	
	MIC $\mu\text{g/mL}$	MBC $\mu\text{g/mL}$	MIC $\mu\text{g/mL}$	MBC $\mu\text{g/mL}$
0.919	1	1	1	1
0.517	1	1	1	1
1.642	-	-	-	-

Ethical approval

This manuscript does not report on or involve the use of any animal or human data or tissue. So the ethical approval is not applicable.

Authors Contributions

All the authors have participated sufficiently in the intellectual content, conception and design of this work or the analysis and interpretation of the data (when applicable), as well as the writing of the manuscript.

Availability of data and materials

Data presented in the manuscript are available via request.

Conflict of Interests

The author declare that they have no known competing financial interests or personal relationships that could have appeared to influence the work reported in this paper.

Open Access

This article is licensed under a Creative Commons Attribution 4.0 International License, which permits use, sharing, adaptation, distribution and reproduction in any medium or format, as long as you give appropriate credit to the original author(s) and the source, provide a link to the Creative Commons license, and indicate if changes were made. The images or other third party material in this article are included in the article's Creative Commons license, unless indicated otherwise in a credit line to the material. If material is not included in the article's Creative Commons license and your intended use is not permitted by statutory regulation or exceeds the permitted use, you will need to obtain permission directly from the OICCPress publisher. To view a copy of this license, visit <https://creativecommons.org/licenses/by/4.0>.

References

- [1] M. Kim, S. Osone, T. Kim, H. Higashi, and T. Seto. "Synthesis of nanoparticles by laser ablation: A review." *KONA Powder Part. J.*, **34**:80–90, 2017. DOI: <https://doi.org/10.14356/kona.2017009>.
- [2] A. Wazeer, A. Das, A. Sinha, and A. Karmakar. "Nanomaterials synthesis via laser ablation in liquid: A review." *J. Inst. Eng. (India): D.*, **104**:413–426, 2023. DOI: <https://doi.org/10.1007/s40033-022-00370-w>.
- [3] L. Malik. "Dark hollow lasers may be better candidates for holography." *Opt. Laser Technol.*, **132**:106485, 2020. DOI: <https://doi.org/10.1016/j.optlastec.2020.106485>.
- [4] N. Ebrahim Jasbi, E. Solati, and D. Dorrnian. "Role of laser fluence in decoration of graphene nanosheets with TiO₂ nanoparticles by pulsed laser ablation method." *J. Alloys Compd.*, **861**:157956, 2021. DOI: <https://doi.org/10.1016/j.jallcom.2020.157956>.
- [5] G. Ferey. "Hybrid porous solids: past, present, future." *Chem Soc Rev.*, **37**:191–214, 2008. DOI: <https://doi.org/10.1039/B618320B>.
- [6] H. Li, M. Eddaoudi, M. O'Keeffe, and O. Yaghi. "Design and synthesis of an exceptionally stable and highly porous metal-organic framework." *Nature*, **402**:276–279, 1999. DOI: <https://doi.org/10.1038/46248>.
- [7] K. Makgopa, M. Ratsoma, and K. D. Modibane. "Intrinsic properties of metal-organic frameworks (MOFs) in supercapacitor applications." *Curr. Opin. Electrochem.*, **36**:101112, 2022. DOI: <https://doi.org/10.1016/j.coelec.2022.101112>.
- [8] Y. Sakamaki, M. Tsuji, Z. Heidrick, O. Watson, J. Durchman, C. Salmon, S. R. Burgin, and H. Beyzavi. "Preparation and applications of metal-organic frameworks (MOFs): A laboratory activity and demonstration for high school and/or undergraduate students." *J. Chem. Educ.*, **97**:1109–1116, 2020. DOI: <https://doi.org/10.1021/acs.jchemed.9b01166>.
- [9] D. Jiang, M. Chen, H. Wang, G. Zeng, D. Huang, M. Cheng, Y. Liu, W. Xue, and Z. W. Wang. "The application of different typological and structural MOFs-based materials for the dye's adsorption." *Coord Chem Rev.*, **380**:471–483, 2019. DOI: <https://doi.org/10.1016/j.ccr.2018.11.002>.
- [10] C. P. Raptopoulou. "Metal-organic frameworks: Synthetic methods and potential applications." *Materials (Basel)*, **14**:310, 2021. DOI: <https://doi.org/10.3390/ma14020310>.
- [11] V. Foziya Yusuf, N. I. Malek, and S. Kumar Kailasa. "Review on metal-organic framework classification, synthetic approaches, and influencing factors: Applications in energy, drug delivery, and wastewater treatment." *ACS Omega.*, **7**:44507–44531, 2022. DOI: <https://doi.org/10.1021/acsomega.2c05310>.
- [12] Z. Hu, B. J. Deibert, and J. Li. "Luminescent metal-organic frameworks for chemical sensing and explosive detection." *Chem Soc Rev.*, **43**:5815–5840, 2014. DOI: <https://doi.org/10.1039/C4CS00010B>.
- [13] L. E. Kreno, K. Leong, O. K. Farha, M. Allendorf, R. P. Van Duyne, and J. T. Hupp. "Metal-organic framework materials as chemical sensors." *Chem Rev.*, **112**:1105–1125, 2012. DOI: <https://doi.org/10.1021/cr200324t>.
- [14] J. Liu, L. Chen, H. Cui, J. Zhang, L. Zhang, and C. Y. Su. "Applications of metal-organic

- frameworks in heterogeneous supramolecular catalysis". *Chem Soc Rev.*, **43**:6011–6061, 2014. DOI: <https://doi.org/10.1039/C4CS00094C>.
- [15] M. P. Suh, H. J. Park, T. K. Prasad, and D. W. Lim. "Hydrogen storage in metal–organic frameworks. ". *Chem Rev.*, **112**:782–835, 2012. DOI: <https://doi.org/10.1021/cr200274s>.
- [16] Y. He, W. Zhou, G. Qian, and B. Chen. "Methane storage in metal–organic frameworks. ". *Chem Soc Rev.*, **43**:5657– 5678, 2014. DOI: <https://doi.org/10.1021/ja4045289>.
- [17] J. R. Li, J. Sculley, and H. C. Zhou. "Metal–organic frameworks for separations.". *Chem Rev.*, **112**:869–932, 2012. DOI: <https://doi.org/10.1021/cr200190s>.
- [18] H. Martínez Pérez-Cejuela, J. Manuel Herrero-Martínez, and E. F. Simó-Alfonso. "Recent advances in affinity MOF-based sorbents with sample preparation purposes.". *Molecules*, **25**:4216, 2020. DOI: <https://doi.org/10.3390/molecules25184216>.
- [19] M. Bazargan, F. Ghaemi, A. Amiri, and M. Mirzaei. "Metal–organic framework-based sorbents in analytical sample preparation.". *Coord. Chem. Rev.*, **445**:214107, 2021. DOI: <https://doi.org/10.1016/j.ccr.2021.214107>.
- [20] H. D. Lawson, S. Patrick Walton, and C. Chan. "Metal–organic frameworks for drug delivery: A design perspective.". *ACS Appl. Mater. Interfaces.*, **13**:7004–7020, 2021. DOI: <https://doi.org/10.1021/acsami.1c01089>.
- [21] S. He, L. Wu, X. Li, H. Sun, T. Xiong, J. Liu, C. Huang, H. Xu, H. Sun, W. Chen, R. Gref, and J. Zhang. "Metal-organic frameworks for advanced drug delivery.". *Acta Pharm. Sin. B.*, **11**:2362–2395, 2021. DOI: <https://doi.org/10.1016/j.apsb.2021.03.019>.
- [22] B. Maranescu and A. Visa. "Applications of metal-organic frameworks as drug delivery systems.". *Int J Mol Sci.*, **23**:4458, 1949. DOI: <https://doi.org/10.3390/ijms23084458>.
- [23] S. Mallakpour, E. Nikkhoo, and C. Mustansar Husain. "Application of MOF materials as drug delivery systems for cancer therapy and dermal treatment.". *Coord. Chem. Rev.*, **451**:214262, 2022. DOI: <https://doi.org/10.1016/j.ccr.2021.214262>.
- [24] L. Yan, A. Gopal, S. Kashif, P. Hazelton, M. Lan, W. Zhang, and X. Chen. "Metal organic frameworks for antibacterial applications.". *J. Chem. Eng.*, **435**:134975, 2022. DOI: <https://doi.org/10.1016/j.ccej.2022.134975>.
- [25] X. Zhang, F. Peng, and D. Wang. "MOFs and MOF-derived materials for antibacterial application. ". *J Funct Biomater.*, **13**:215, 2022. DOI: <https://doi.org/10.3390/jfb13040215>.
- [26] D. Han, X. Liub, and S. Wu. "Metal organic framework-based antibacterial agents and their underlying mechanisms.". *Chem. Soc. Rev.*, **51**:7138–7169, 2022. DOI: <https://doi.org/10.1039/D2CS00460G>.
- [27] L. Hashemi, M. Y. Masoomi, and H. Garcia. "Regeneration and reconstruction of metal-organic frameworks: Opportunities for industrial usage. ". *Coord. Chem. Rev.*, **472**:214776, 2022. DOI: <https://doi.org/10.1016/j.ccr.2022.214776>.
- [28] Y. Li, G. Wen, J. Li, Q. Li, H. Zhang, B. Taoa, and J. Zhang. "Synthesis and shaping of metal–organic frameworks: A review.". *Chem. Commun.*, **58**:11488–11506, 2022. DOI: <https://doi.org/10.1039/D2CC04190A>.
- [29] N. Stock and S. Biswas. "Synthesis of metal-organic frameworks (MOFs): Routes to various MOF topologies, morphologies, and composites.". *Chem. Rev.*, **112**:933–969, 2012. DOI: <https://doi.org/10.1021/cr200304e>.
- [30] T. D. Bennett, Y. Yue, P. Li, A. Qiao, H. Tao, N. G. Greaves, T. Richards, G. I. Lampronti, Simon A. T. Redfern, F. Blanc, O. K. Farha, et al. "Melt-quenched glasses of metal–organic frameworks.". *J. Am. Chem. Soc.*, **138**:3484–3492, 2016. DOI: <https://doi.org/10.1021/jacs.5b13220>.
- [31] B. Chen, Z. Yang, Y. Zhua, and Y. Xia. "Zeolitic imidazolate framework materials: recent progress in synthesis and applications.". *J. Mater. Chem. A.*, **2**:16811–16831, 2014. DOI: <https://doi.org/10.1039/C4TA02984D>.
- [32] S. Kouser, A. Hezam, M. J. N. Khadri, and S. Ara Khanum. "A review on zeolite imidazole frameworks: synthesis, properties, and applications.". *J. Porous Mater.*, **29**:663–681, 2022. DOI: <https://doi.org/10.1007/s10934-021-01184-z>.
- [33] D. J. Tranchemontagne, R. J. Hunt, and O. Yaghi. "Room temperature synthesis of metal-organic frameworks: MOF-5, MOF-74, MOF-177, MOF-199, and IRMOF-0. ". *Tetrahedron*, **64**:8553–8557, 2008. DOI: <https://doi.org/10.1016/j.tet.2008.06.036>.
- [34] B. Zhang, Y. Luo, K. Kanyuck, N. Saenz, K. Reed, P. Zavalij, J. Mowery, and G. Bauchan. "Facile and template-free solvothermal synthesis of mesoporous/macroporous metal–organic framework nanosheets.". *RSC Adv.*, **8**:33059–33064, 2018. DOI: <https://doi.org/10.1039/C8RA06576D>.
- [35] T. Sattar and M. Athar. "Hydrothermal synthesis and characterization of copper glycinate (Bio-MOF-29) and it's in vitro drugs adsorption studies.". *J Inorg Chem.*, **7**:17–27, 2017. DOI: <https://doi.org/10.4236/ojic.2017.72002>.
- [36] J. H. Liao, P. C. Wu, and W. C. Huang. "Ionic liquid as solvent for the synthesis and crystallization of

- a coordination polymer: (EMI)[Cd(BTC)] (EMI = 1-Ethyl-3-methylimidazolium, BTC = 1,3,5-benzenetricarboxylate)". *Cryst Growth Des.*, **6**:1062–1063, 1988. DOI: <https://doi.org/10.1021/cg0504197>.
- [37] J. K. Choi, J. Kim, S. H. Jhung, H. K. Kim, J. S. Chang, and H. K. Chae. "Microwave synthesis of a porous metal organic framework: zinc terephthalate MOF-5". *Bull Kor Chem Soc.*, **27**:1523–1524, 2006. DOI: <https://doi.org/10.5012/bkcs.2006.27.10.1523>.
- [38] S. H. Jhung, J. H. Lee, J. W. Yoon, C. Serre, G. Ferey, and J. S. Chang. "Microwave synthesis of chromium terephthalate MIL-101 and Its benzene sorption". *Adv Mater.*, **19**:121–124, 2007. DOI: <https://doi.org/10.1002/adma.200601604>.
- [39] W. J. Son, J. Kim, J. Kim, and W. S. Ahn. "Sonochemical synthesis of MOF-5". *Chem Commun.*, **47**:6336–6338, 2008. DOI: <https://doi.org/10.1039/B814740J>.
- [40] Y. Chen, C. Yang, X. Wang, J. Yang, K. Ouyang, and J. Li. "Kinetically controlled ammonia vapor diffusion synthesis of a Zn(II) MOF and its H₂O/NH₃ adsorption properties". *J Mater Chem A.*, **4**:10345–10351, 2016. DOI: <https://doi.org/10.1039/C6TA03314H>.
- [41] H. M. Yang, X. Liu, X. L. Song, T. L. Yang, Z. H. Liang, and C. M. Fan. "In situ electrochemical synthesis of MOF-5 and its application in improving photocatalytic activity of BiOBr". *Transactions of Non-ferrous Metals Society of China*, **25**:3987–3994, 2015. DOI: [https://doi.org/10.1016/S1003-6326\(15\)64047-X](https://doi.org/10.1016/S1003-6326(15)64047-X).
- [42] D. Lv, Y. Chen, Y. Li, R. Shi, H. Wu, X. Sun, J. Xiao, H. Xi, Q. Xia, and Z. Li. "Efficient mechanochemical synthesis of MOF-5 for linear alkanes adsorption". *J. Chem Eng Data.*, **62**:2030–2036, 2017. DOI: <https://doi.org/10.1021/acs.jced.7b00049>.
- [43] S. L. Campello, G. Gentil, S. A. Júnior, and W. M. de Azevedo. "Laser ablation: a new technique for the preparation of metal-organic frameworks Cu₃(BTC)₂(H₂O)₃". *Mater.*, **148**:200–203, 2015. DOI: <https://doi.org/10.1016/j.matlet.2015.01.159>.
- [44] O. Maria Menezes Madeiro da Costa and W. M. de Azevedo. "Highly luminescent metal organic framework Eu (TMA)(H₂O)₄ materials prepared by laser ablation technique in liquid". *J Lumin.*, **170**:648–653, 2016. DOI: <https://doi.org/10.1016/j.jlumin.2015.09.004>.
- [45] E. L. Ribeiro, S. A. Davari, S. Hu, D. Mukherjee, and B. Khomami. "Laser-induced synthesis of ZIF-67: A facile approach for the fabrication of crystalline MOFs with tailored size and geometry". **3**:1302–1309, 2019. DOI: <https://doi.org/10.1039/C8QM00671G>.
- [46] R. Sabouni, H. Kazemian, and S. Rohani. "A novel combined manufacturing technique for rapid production of IRMOF-1 using ultrasound and microwave energies". *Chem Eng J.*, **165**:966–973, 2010. DOI: <https://doi.org/10.1016/j.cej.2010.09.036>.
- [47] Y. R. Lee, M. S. Jang, H. Y. Cho, H. J. Kwon, S. Kim, and W. S. Ahn. "ZIF-8: A comparison of synthesis methods". *J. Chem. Eng.*, **271**:276–280, 2015. DOI: <https://doi.org/10.1016/j.cej.2015.02.094>.
- [48] R. Banerjee, A. Phan, B. Wang, C. Knobler, H. Furukawa, M. O’Keeffe, and O. M. Yaghi. "High-throughput synthesis of zeolitic imidazolate frameworks and application to CO₂ capture". *Science*, **319**:939–943, 2008. DOI: <https://doi.org/10.1126/science.1152516>.
- [49] K. S. Park, Z. Ni, A. P. Côté, J. Y. Choi, R. Huang, F. J. Uribe-Romo, H. K. Chae, M. O’Keeffe, and O. M. Yaghi. "Exceptional chemical and thermal stability of zeolitic imidazolate frameworks". *Proc. Natl. Acad. Sci.*, **103**:10186–10191, 2006. DOI: <https://doi.org/10.1073/pnas.0602439103>.
- [50] Z. Jiang, M. Zhang, X. Chen, B. Wang, W. Fan, C. Yang, X. Yang, Z. Zhang, X. Yang, C. Li, and T. Zhou. "A bismuth-based zeolitic organic framework with coordination-linked metal cages for efficient electrocatalytic CO₂ reduction to HCOOH". *Angew. Chem.*, **62**:e202311223, 2023. DOI: <https://doi.org/10.1002/anie.202311223>.
- [51] F. Ataei, D. Dorrnian, and N. Motakef-Kazemi. "Synthesis of MOF-5 nanostructures by laser ablation method in liquid and evaluation of its properties". *J Mater Sci Mater Electron.*, **32**:3819, 2021. DOI: <https://doi.org/10.1007/s10854-020-05126-4>.
- [52] N. Motakef-Kazemi, F. Ataei, and D. Dorrnian. "Laser ablation produced graphene/MOF-5 nanocomposite: antibacterial properties". *JTAP.*, **17**:1–9, 2023. DOI: <https://doi.org/10.57647/j.jtap.2023.1701.09>.
- [53] F. Ataei, D. Dorrnian, and N. Motakef-Kazemi. "Bismuth-based metal-organic framework prepared by pulsed laser ablation method in liquid". *Phys. Lett. A*, **14**:1–8, 2020. DOI: <https://doi.org/10.1007/s40094-020-00397-y>.
- [54] E. L. Ribeiro, S. A. Davari, S. Hu, D. Mukherjee, and B. Khomami. "Laser-induced synthesis of ZIF-67: a facile approach for the fabrication of crystalline MOFs with tailored size and geometry". *Mater Chem Front.*, **3**:1302, 2019. DOI: <https://doi.org/10.1039/C8QM00671G>.
- [55] N. Motakef-Kazemi, F. Ataei, and D. Dorrnian. "Synthesis and evaluation of copper-imidazole MOF nanostructures and its graphene nanocomposites by pulsed laser ablation method in liquid". *Opt Quantum Electron.*, **55**:921, 2023. DOI: <https://doi.org/10.1007/s11082-023-04775-z>.
- [56] N. Nagarjun and A. Dhakshinamoorthy. "A Cu-Doped ZIF-8 metal organic framework as a heterogeneous

solid catalyst for aerobic oxidation of benzylic hydrocarbons”. *New J Chem.*, **43**:18702–18712, 2019. DOI: <https://doi.org/10.1039/C9NJ03698A>.

- [57] M. Yahia, Q. Nhu Phan Le, N. Ismail, M. Essalhi, O. Sundman, A. Rahimpour, M. M. Dal-Cin, and N. Tavajohi. “Effect of incorporating different ZIF-8 crystal sizes in the polymer of intrinsic microporosity, PIM-1, for CO₂/CH₄ separation.”. *Micropor Mesopor Mat.*, **312**:110761, 2021. DOI: <https://doi.org/10.1016/j.micromeso.2020.110761>.
- [58] A. Sirelkhatim, S. Mahmud, A. Seeni, N. H. M. Kaus, L. C. Ann, S. K. M. Bakhori, H. Hasan, and D. Mohamad. “Review on zinc oxide nanoparticles: antibacterial activity and toxicity mechanism.”. *Nano-Micro Lett.*, **7**:219–242, 2015. DOI: <https://doi.org/10.1007/s40820-015-0040-x>.